 doi:10.20944/preprints202009.0660.v1

Article

Mechanochemical synthesis and structure of the tetrahydrate and mesoporous anhydrous metforminium(2+)-*N,N'*-1,4-phenylenedioxalamic acid cocrystal salt: the role of hydrogen bonding and n→π* charge assisted interactions

Sayuri Chong-Canto [1], Efrén V. García-Báez [1], Francisco J. Martínez-Martínez [2], Angel A. Ramos-Organillo [2], Itzia I. Padilla-Martínez [1*]

[1] Laboratorio de Química Supramolecular y Nanociencias, Instituto Politécnico Nacional-UPIBI, Av. Acueducto s/n Barrio la Laguna Ticomán, Ciudad de México, C.P. 07340, Mexico; anothersayuri2341@gmail.com (S.C.-C); ipadillamar@ipn.mx (I.I.P.-M.); egarciab@ipn.mx (E.V.G.-B.).

[2] Facultad de Ciencias Químicas, Universidad de Colima, Km. 9 Carretera Colima-Coquimatlán, C.P. 28400, Coquimatlán, Colima, Mexico; fjmartin@ucol.mx (F.J.M.-M.); aaramos@ucol.mx (A.A.R.-O.)

* Correspondence: ipadillamar@ipn.mx; Tel.: +52-555-729-6000 (ext. 56324)

Received: date; Accepted: date; Published: date

Abstract: A new cocrystal salt of metformin, an antidiabetic drug, and *N,N'*-(1,4-phenylene)dioxalamic acid, was synthesized by mechanochemical synthesis, purified by crystallization from solution and characterized by single X-ray crystallography. The structure revealed a salt-type cocrystal composed of one dicationic metformin unit, two monoanionic units of the acid and four water molecules namely $H_2Mf(HpOXA)_2{\cdot}4H_2O$. X-ray powder, IR, ^{13}C-CPMAS, thermal and BET adsorption-desorption analyses were performed to elucidate the structure of the molecular and supramolecurar structure of the anhydrous microcrystalline mesoporous solid $H_2Mf(HpOXA)_2$. The results suggest that their structures, conformation and hydrogen bonding schemes are very similar between them. To the best of our knowledge, the selective formation of the monoanion $HpOXA^-$, as well as its structure in the solid, is herein reported for the first time. Regular O(δ-)···C(δ+), O(δ-)···N^+ and bifacial O(δ-)···C(δ+)···O(δ-) of n→π* charge-assisted interactions are herein described in H_2MfA cocrystal salts which could be responsible of the interactions of metformin in biologic systems. The results, support the participation of n→π* charge-assisted interactions independently, and not just as a short contact imposed by the geometric constraint due to the hydrogen bonding patterns.

Keywords: metformin cocrystal, mechanochemical synthesis, dicationic metformin, water channels, pi-interactions, mesoporous anhydrate.

1. Introduction

Cocrystallization has become a growing discipline of interest in pharmaceutical sciences, since it has been demonstrated its application to modify the physical-chemical properties of known drugs [1]. Metformin-HCl (HMfCl) is an oral anti-hyperglycemic drug, worldwide used for the treatment of non-insulin dependent diabetes mellitus. It improves glucose tolerance lowering plasma glucose levels and glycated hemoglobin, particularly in overweight and obese patients. Metformin is one of the most frequently small molecules used to prepare combined drugs such as Segluromet (metformin-ertugliflozin), Metaglip (metformin-glipizide) and Glucovance (metformin-glyburide). These are examples of the fourteen combinations approved by FDA [2], some of them have been

 doi:10.20944/preprints202009.0660.v1

characterized by monocrystal X-ray diffraction such as metformin-glimepiride [3] and metformin-salicylic acid [4]. Due to its pharmaceutical importance, there is a great interest in metformin cocrystals, that has led to several patents related to the formation of organic salts, compiled elsewhere [5].

In addition, the structure and electronic structural details on metformin and its cocrystals has been recently summarized, in the context of biguanide compounds [6]. Metformin is a privileged small molecule; it possesses conformational flexibility and is capable to form strong hydrogen bonding interactions which will determine its structure and activity in biological processes. Metformin hydrochloride is known to crystallize in two conformational polymorphs namely A [7] and B [8]. The $Me_2N—C—N—C$ backbone adopts the U conformation in the thermodynamic phase A (Me_2NCNC torsion angle value of 53.7°), whereas the form of an S backbone is observed in the metastable polymorph B (Me_2NCNC torsion angle value of 129.1°). The calculated minima are near 50° and 160°, respectively [9].

On the other hand, oxalamic or oxamic acids are the amide-carboxylic acid derivatives of the oxalic acid. They have been recognized because of their high potential in crystal engineering and molecular recognition due to their bifunctionality [10]. As far as and N,N′-(1,4-phenylene)dioxalamic acid (H_2pOXA) is concerned and its 1,3-isomer (H_2mOXA), they were first reported in the mid 70´s [11, 12] as antiallergic agents as well as anti-inflammatory compounds [13]. More recently, both have attracted interest as coordinating ligands for metals [14, 15]. Theoretical studies and experimental work [16] have demonstrated the high flexibility of the oxalic acid derivatives. Both oxalyl carbonyls are usually in anti disposition [17] but they less frequently adopt the syn disposition, induced by steric constraints [18, 19] or by coordination with metals in the form of carboxylates [14].

Finally, mechanochemical synthesis consists of the application of mechanical energy to induce a chemical reaction, its use and applications have been recently reviewed [20]. Liquid-assisted grinding (LAG) makes use of some drops of solvent to provide greater molecular mobility in the course of the milling procedure. Even though the liquid does not play the role of solvent, it can be incorporated into the crystal network to form solvates or not.

Herein we report, the LAG method to synthesize the tetrahydrate and anhydrate of the antidiabetic drug metformin and *N,N′*-(1,4-phenylene)dioxalamic acid. Their molecular and supramolecular structures were analyzed in the context of the interactions of metformin in biologic systems.

2. Materials and Methods

Materials and crystal synthesis. Metformin hydrochloride (HMetCl) was isolated from commercial sources: 10 tablets of 500 mg were grinded and suspended in 150 mL of ethyl alcohol (96%), the mixture was boiled under stirring for 10 min or until complete dissolution. The hot solution was filtered; crystals of HMfCl were obtained after cooling to room temperature to obtain 2.5 g of a white solid, which was analyzed by IR, NMR and single crystal X-ray diffraction, corresponding to the crystal structure reported by Hariharan [7]. The *N,N′*-(1,4-phenylene)dioxalamic acid double hydrate (H_2pOXA·2W, W = water) was obtained as reported elsewhere [14]. Single crystals of *N,N′*-(1,4-phenylene)dioxalamate of di-(metformin diammonium) tetrahydrate (H_2Mf(HpOXA)$_2$·4W) were synthesized starting from 0.060 g (0.350 mmol) of HMfCl and 100 mg (0.347 mmol) H_2pOXA·2W which were grinded with a pestle in a mortar with the aid of few drops of water for 33-45 min until a homogeneous paste was formed. This mass was suspended in 40 mL of water and boiled under stirring until a clear solution appeared. The solution was left to stand at room temperature and after two days, 0.113 g (0.16 mmol) of beige crystals suitable for X-ray analysis were obtained in 92% yield. Similar results were obtained using 1:2 stoichiometric amounts of HMfCl (0.030 mg) to H_2pOXA·2W (100 mg) to obtain 0.120 g (0.17 mmol) of H_2Mf(HpOXA)$_2$·4W in 98% yield. Microcrystalline powder of H_2Mf(HpOXA)$_2$ was obtained from single crystals of H_2Mf(HpOXA)$_2$·4W after drying at 100 °C for 2 h in an air oven.

Preprints (www.preprints.org) | NOT PEER-REVIEWED | Posted: 27 September 2020 doi:10.20944/preprints202009.0660.v1

Instrumental. IR spectra were recorded neat at 25 °C using a Perkin Elmer Spectrum GX series with FT system spectrophotometer using the ATR device. ^{13}C-CPMAS spectra were recorded on a Bruker Avance DPX-400 (101 MHz). The following conditions were applied: spectral width 30.242 kHz, acquisition time 33.8 ms, contact time 2000 ms, rotation rate 8 kHz, relaxation delay 5 s, and up to 256 scans for each spectrum were collected. Room temperature X-ray powder diffraction data were collected on a PAN Analytical X'Pert PRO diffractometer with Cu Kα1 radiation (λ = 1.5405 Å, 45 kV, 40 mA) or on a D8 Focus Bruker AXS instrument using Cu Kα1 radiation (λ = 1.542 Å, 35 kV, 25 mA). Texture analysis of $H_2Mf(HpOXA)_2$ was performed using 0.0408 g of sample in an ASAP-2050 Xtended Pressure Sorption Analyzer of Micromeritics using liquid nitrogen. DSC and TG measurements were performed in a Q2000 equipment and a Thermobalance Q5000 IR, respectively, of TA instruments. In both cases, approximately 3.0-5.0 mg of sample was used and a gradient of 5.00 °C/min from room temperature to 350 °C under air flux of 25 mL/min in an open (TG) or pin-holed panels (DSC).

X-Ray structure determination. General crystallographic data for $H_2Mf(HpOXA)_2{\cdot}4W$ has been deposited in the Cambridge Crystallographic Data Centre (CCDC) as supplementary publication number 1874280. Single crystal X-ray diffraction data was collected on an Agilent SuperNova (dual source) diffractometer using graphite-monochromatic Mo (λ = 0.71073 Å) Kα radiation; data collection, cell refinement and data reduction were accomplished using CrysAlisPro software [21]. The structure was solved by direct methods using the SHELXS-97 program [22] of the WINGX package [23]. The final refinement was performed by full-matrix least-squares methods using the SHELX97 program[22]. The H atoms on C, N, and O were geometrically positioned and treated as riding atoms with: C−H 0.93−0.98 Å, Uiso(H) = 1.2 eq(C) for aromatic carbon atoms or 1.5 eq(C) for methyl carbon atoms; O−H = 0.82 Å, Uiso(H) = 1.5 eq(O); N−H = 0.86 Å, Uiso(H) = 1.2 eq(N). Platon [24] and Mercury [25] were used to prepare the material for publication.

Crystal Data for $2(C_{10}H_7N_2O_6){\cdot}(C_4H_{13}N_5){\cdot}4(H_2O)$, ($H_2Mf(HpOXA)_2{\cdot}4W$), M = 705.61 g/mol: triclinic, space group *P*-1, a = 8.1357 (11), b = 13.8594 (18), c = 14.4846 (13) Å, α = 109.963 (10)°, β = 92.453 (9)°, γ = 95.863 (11)°, V = 1521.8 Å^3, Z = 2, T = 293 K, μ(MoKα) = 0.71073 Å, Dcalc = 1.540 g/cm^3, 10559 reflections measured (3.0° ≤ 2Θ ≤ 52.57°), 5942 unique (Rint = 0.027, Rsigma = 0.034) which were used in all calculations. The final R1 was 0.047 (I > 2σ(I)) and wR2 was 0.1400 (all data).

3. Results and discussion

3.1. Synthesis

Microcrystalline solid phase of *N,N'*-(1,4-phenylene)dioxalamate of di-(metformin diammonium) tetrahydrate ($H_2Mf(HpOXA)_2{\cdot}4W$) were synthesized using water-assisted grinding procedure. Two stoichiometric proportions were used of HMfCl/H_2pOXA: 1:1 and 1:2. In both cases, the reaction was monitored to completion by comparing the XRPD patterns of the mixtures to the pristine HMfCl, Figure 1. Single crystals of $H_2Mf(HpOXA)_2{\cdot}4W$ cocrystal salt were obtained by recrystallization from hot water of either of the two grinded mixtures. The reaction is quantitative based on the stoichiometry of the following reaction:

$$2HMf^{+} + 2H_2pOXA + 4H_2O \rightarrow H_2Mf^{2+} + H_2Mf(HpOXA)_2{\cdot}4H_2O$$

The proton of one carboxylic acid group of H_2pOXA is transferred to the remaining basic nitrogen site of HMfCl molecule to form the H_2Mf^{2+} dication and the monoanion of *N,N'*-(1,4-phenylene)dioxalamic acid ($HpOXA^-$), which crystallize from the aqueous solution as $H_2Mf(HpOXA)_2{\cdot}4W$ cocrystal salt. Therefore, even when it can be obtained by milling procedure in the solid state, the crystallization step from aqueous solution is required in order to eliminate the remaining H_2MfCl_2 byproduct.

Microcrystalline powder of $H_2Mf(HpOXA)_2$ was obtained from single crystals of $H_2Mf(HpOXA)_2{\cdot}4W$ after drying at 100 °C for 2 h in an air oven.

Preprints (www.preprints.org) | NOT PEER-REVIEWED | Posted: 27 September 2020 doi:10.20944/preprints202009.0660.v1

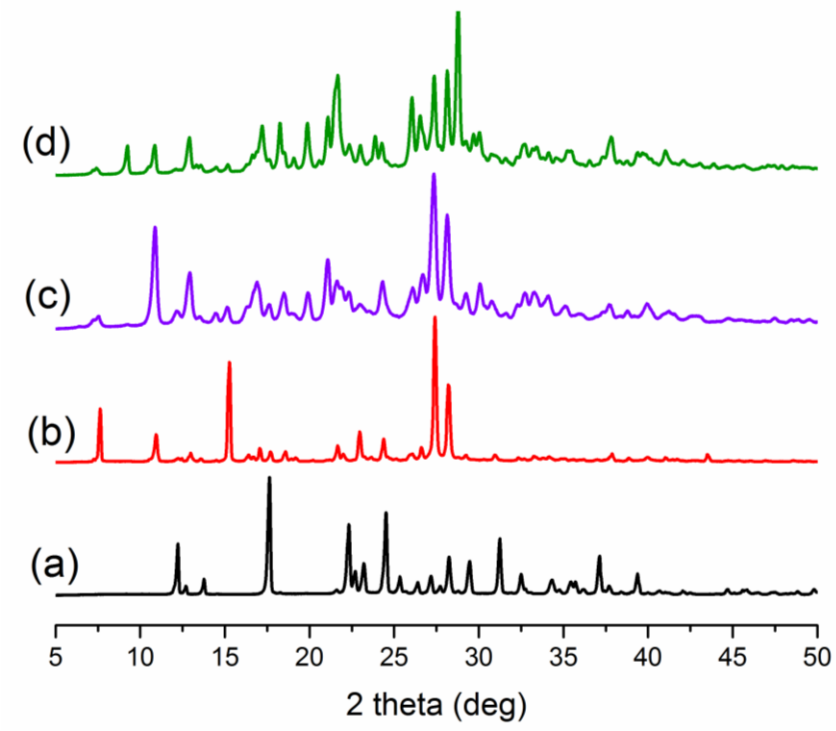

Figure 1. XRPD patterns of: (a) pristine HMfCl, (b) $H_2Mf(HpOXA)_2{\cdot}4W$ cocrystal salt (experimental), (c) mechanochemical synthesis in 1:1 proportion of HMfCl/H_2pOXA and (d) mechanochemical synthesis in 1:2 proportion of HMfCl/H_2pOXA.

3.2. The molecular and supramolecular structure of $H_2Mf(HpOXA)_2{\cdot}4W$.

The cocrystal salt $H_2Mf(HpOXA)_2{\cdot}4W$ crystallizes in the triclinic system, space group *P*-1 with one, two and four independent units of H_2Mf^{2+}, $HpOXA^-$ and H_2O in the asymmetric unit, respectively, and whose molecular structure is depicted in Figure 2.

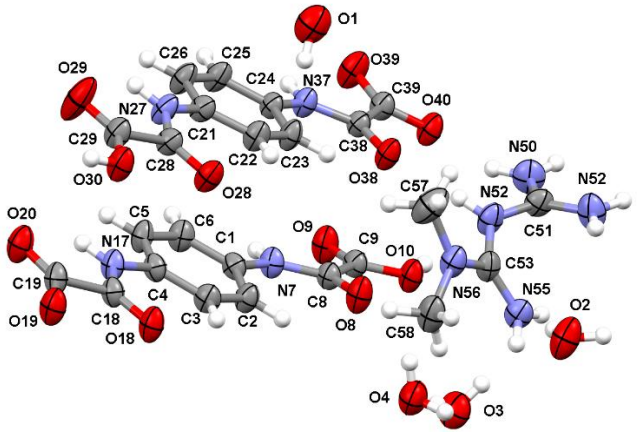

Figure 2. Molecular structure of the cocrystal salt $H_2Mf(HpOXA)_2{\cdot}4W$ showing the atom labelling scheme. Displacement ellipsoids are drawn at the 50% probability level.

The oxalyl fragments COCO are almost planar, with a mean O—C—C—O angle of 179.3(6)°. However, small differences can be noted between the oxalamic acid $NCOCO_2H$ and oxalamate fragments, $NCOCO_2^-$. The $NCOCO_2H$ endings are located slightly out of plane of the corresponding benzene ring, the maximum deviations from planarity are presented by N7C8O8C9O9O10H10 and N27C28O28C29O29O30H30 fragments with torsion angles of 16.08(5)° and 9.83(6)° from the C1-C6 and C21-C26 rings, respectively. Instead, the oxalamate counterparts $NCOCO_2^-$ are almost coplanar to the corresponding benzene ring: 3.50(6)° for N17C18O18C19O19O20 and 5.02(6)° for

Preprints (www.preprints.org) | NOT PEER-REVIEWED | Posted: 27 September 2020 doi:10.20944/preprints202009.0660.v1

N37C38O38C239O39O40. It is worth to note that $NCOCO_2H$ and $NCOCO_2^-$ arms are in *syn* disposition between each other (*sp-sp* conformation). It is worth to mention that this conformation has not been observed among organic cocrystals of H_2pOXA but is commonly attained by coordination to metals [26]. The calculated conformational landscape of 1,4-phenylen dioxalyls predicts a very small difference in energy between planar *ap-sp* and *sp-sp* conformers of 0.26-0.28 kcal mol^{-1}, in favor of the former, and an interconversion energy of only 4.80 kcal mol^{-1} [16]. Then, the *sp-sp* conformation exhibited by the $HpOXA^-$ moiety is explained because of the stabilization given by hydrogen bonding with metformin that provides the energy to overcome the rotational barrier.

The C(*sp*²)—N(*sp*²) bond lengths of the metformin dication moiety range from 1.302(3) to 1.378(3) Å. In fact, the bond lengths of C52 and C54 with the terminal nitrogen atoms are shorter, whereas the corresponding bond lengths with the bridge N53 atom are longer, than those bonds observed in monocationic metformin (1.333–1.341 Å) [27]. These last bond lengths have values close to those observed in five membered heterocycles involving pyrrolic nitrogen (≈ 1.37 Å) [28]. In agreement, the proposed delocalized structure is depicted in Figure 3. Selected bond lengths and torsion angles are listed in Table 1. In $H_2Mf(HpOXA)_2{\cdot}4W$, the two planar guanidinium halves N53C54N55N56 and N53C52N51N50, are twisted by 55.67(9)° and the NMe_2 group is located opposite to the $C(NH_2)_2$ group (N56C54N53C52 torsion angle value of 148.8(2)°).

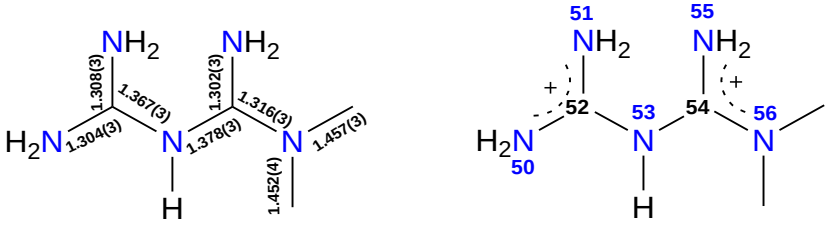

Figure 3. Bond lengths in Å (left) and delocalized structure of the dicationic metformin H_2Mf^{2+} (right) showing the atom numbering scheme.

In the cocrystal salt $H_2Mf(HpOXA)_2{\cdot}4W$, the metforminium moiety adopts the S backbone conformation which has been reported as the most stable owing to the decreased van der Waals repulsion, greater π-electron delocalization and intramolecular hydrogen bonding [9]. The structure of metformin in the cocrystal salt $H_2Mf(HpOXA)_2{\cdot}4W$ is very similar to that observed in the monohydrates of dicationic 1:1 salts of formula $H_2MfA{\cdot}H_2O$ (A = oxalate, sulfate) [29] supporting that the anions slightly influence the structure of *N,N*-dimethylbiguanidinium moiety.

Table 1. Selected bond lengths and torsion angles of the cocrystal salt $H_2Mf(HpOXA)_2{\cdot}4W$.

		$HpOXA^-$ moiety	
Atoms	**Bond Lengths/Å**	**Atoms**	**Bond Lengths/Å**
C8—C9	1.534(3)	C18—C19	1.556(3)
C28—C29	1.542(3)	C38—C39	1.550(3)
	Torsion angles/°		**Torsion angles/°**
C2—C1—N7—C8	-16.7(4)	C3—C4—N17—C18	-2.7(4)
O8—C8—N7—C1	1.5(4)	O8—C8—C9—O9	-179.7(2)
O18—C18—N17—C4	1.1(4)	O18—C18—C19—O19	177.0(2)
C22—C21—N27—C28	-11.1(4)	C23—C24—C25—C26	-1.1(3)
O28—C28—N27—C21	2.4(4)	O28—C28—C29—O29	-178.8(2)
O28—C28—N27—C21	2.4(4)	O28—C28—C29—O29	-178.8(2)
O38—C38—N37—C24	4.8(4)	O38—C38—C39—O39	-171.6(2)
		H_2Mf^{2+} moiety	
Atoms	**Bond Lengths/Å**	**Atoms**	**Bond Lengths/Å**
N50—C52	1.304(3)	N51—C52	1.308(3)

Preprints (www.preprints.org) | NOT PEER-REVIEWED | Posted: 27 September 2020 doi:10.20944/preprints202009.0660.v1

N53—C52	1.367(3)	N53—C54	1.378(3)
N55—C54	1.302(3)	N56—C54	1.316(3)
N56—C58	1.457(3)	N56—C57	1.452(4)
Torsion angle/°			
N56—C54—N53—C52	148.8(2)		

The H_2Mf^{2+} and both $HpOXA^-$ moieties are attached to each other through N53–H53···O38 and N50–H50A···O40 which lead to $R^2_2(9)$ hydrogen bonding ring motif and N51–H51B···O18 hydrogen bonding interactions. Four water molecules, forming amide···water interactions of bifurcated type in $R^1_2(6)$ ring motif (Nn–Hn···Om···Hp—Cp; n = 7, 17; m = 3, 1; p = 6, 5), water···carboxylate (O2–H2B···O19$^-$) and water···water (O3–H3A···O4) hydrogen bonding interactions, complete this basic repetition unit, Figure 4(a). A duplex is formed by an inversion center of symmetry linked by N55–H55B···O28 hydrogen bonding, Figure 5(b), n→π* charge assisted interactions between O8···C54···O18, O8···N56, Figure 4(b) and several CO···CO interactions of sheared parallel type [30]. The geometric parameters associated to these interactions are listed in Table 2. Double strands are generated through acid···carboxylate (On–Hn···Om$^-$; n =10, 30; m = 40, 20) and N50–H50B···O9 hydrogen bonding, Figure 5(a). Whereas the second dimension is developed by water···$HpOXA^-$ interactions (On–Hn···Om$^-$; n = 2, 4; m = 39, 29), N37–H37···O1 and N55–H55A···O2, to form double layers within the (1 1 -1) plane, Figure 5(b). A view, along the perpendicular direction to this plane, let us to note two well-defined regions of metformin and water, Figure 4(c). The distance between two $HpOXA^-$ chains is longer in the metformin region than in the water region, in order to accommodate the NMe_2 group, with mean values of 7.4(3) Å and 4.1(3) Å, respectively (distances measured between benzene ring edges). Finally, water molecules link the bilayers to develop the third dimension along the [0 1 1] direction (N27–H27···O2, N50–H50B···O4, N51–H51A···O4, O1–H1A···O3, O1–H1B···O19, O3–H3B···O39, O4–H4A···O8 and O4–H4A···O10). The water molecules labelled as H_2O1 (W1), H_2O3 (W3) and H_2O4 (W4) form an open cluster, but together with H_2O2 (W2) are located in isolated pockets of the crystal lattice. The geometric parameters associated with intermolecular hydrogen bonding are listed in Table 3.

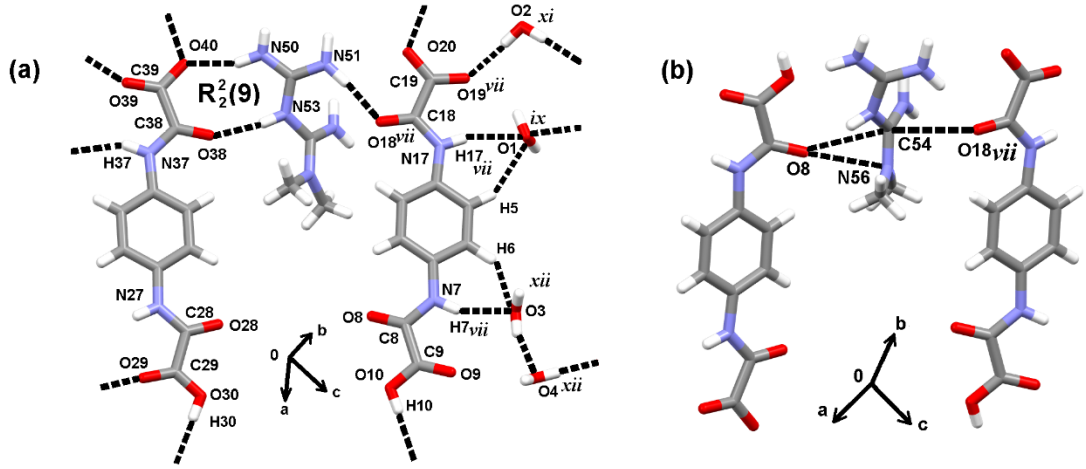

Figure 4. (a) Basic repetition unit of the cocrystal salt $H_2Mf(HpOXA)_2{\cdot}4W$ and atom labelling scheme. (b) n→π* charge-assisted interactions between O8···C54···O18 and O8···N56 that contribute to form the duplex by an inversion center of symmetry. See Tables 2 and 3 for symmetry codes.

Table 2. Geometric parameters of CO···A interactions (A = CO, N) in $H_2Mf(HpOXA){\cdot}4W$..

C—O···A	C—O/Å	O···A/Å	C—O···A/°
C38—O38···C9	1.219(2)	3.083(3)	89.0(2)
C38—O38···C8	1.219(2)	3.075(3)	102.1(2)
C29—O30···C19	1.264(3)	3.198(3)	97.4(2)

Preprints (www.preprints.org) | NOT PEER-REVIEWED | Posted: 27 September 2020 doi:10.20944/preprints202009.0660.v1

C8—O8···C54	1.222(2)	3.142(3)	133.4(2)
C8—O8···N56	1.222(2)	3.003(3)	143.6(2)
C18—O18^{vii}···C54	1.222(3)	3.109(3)	131.8(2)

(vii) −*x*+1, −*y*+1,-*z*+1

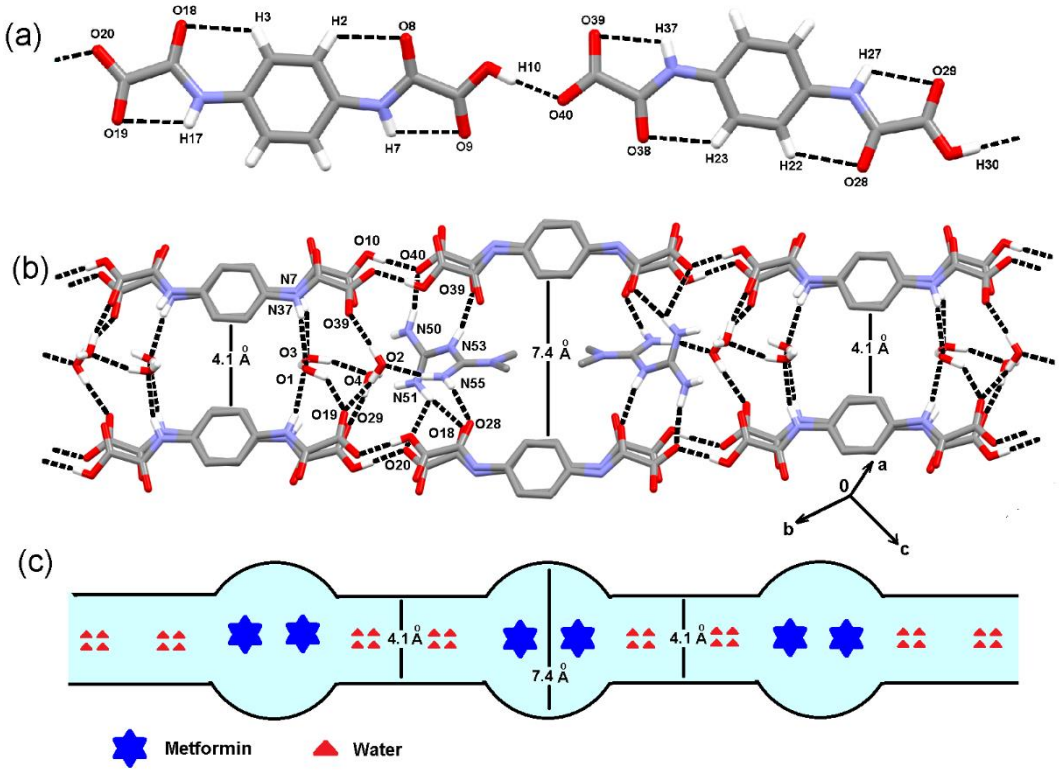

Figure 5. (a) Acid···carboxylate hydrogen bonding between the two units of $HpOXA^-$. (b) Double strands of $H_2Mf(HpOXA)_2{\cdot}4W$ propagating along the (1 1 -1) plane. (c) Pictorial representation of $H_2Mf(HpOXA)_2{\cdot}4W$ where metformin diammonium and water pockets are highlighted.

Table 3. Intermolecular hydrogen bonding geometric parameters of $H_2Mf(HpOXA)_2{\cdot}4W$.

D—H···*A*	*D*—H/Å	H···*A*/Å	*D*···*A*/Å	*D*—H···*A*/°
C5—H5···O1^{i}	0.93	2.62	3.438 (3)	147
C6—H6···O3^{ii}	0.93	2.48	3.217 (3)	136
N7—H7···O3^{ii}	0.86	2.17	2.991 (2)	159
N17—H17···O1^{i}	0.86	2.37	3.208 (3)	166
N27—H27···O2^{iii}	0.86	2.58	3.154 (3)	125
N37—H37···O1^{iv}	0.86	2.49	3.185 (3)	139
N50—H50B···O40	0.86	2.02	2.820 (3)	154
N50—H50*A*···O4^{v}	0.86	2.27	2.999 (3)	143
N50—H50*A*···O9^{vi}	0.86	2.37	2.982 (2)	129
N51—H51*A*···O4^{v}	0.86	2.20	2.947 (3)	145
N51—H51*B*···O18^{vii}	0.86	2.10	2.918 (2)	159
N53—H53···O38	0.86	2.00	2.843 (2)	168
N55—H55*A*···O2	0.86	1.92	2.730 (2)	157
N55—H55*B*···O28^{vii}	0.86	2.05	2.832 (2)	151
O1—H1*A*···O3^{vii}	0.85	2.15	2.985 (3)	169
O1—H1*B*···O19^{i}	0.85	2.33	2.998 (3)	136
O2—H2*A*···O39^{vi}	0.85	1.89	2.742 (2)	177

Preprints (www.preprints.org) | NOT PEER-REVIEWED | Posted: 27 September 2020 doi:10.20944/preprints202009.0660.v1

O2—H2*B*···O19^{viii}	0.85	1.93	2.760 (2)	166
O3—H3*A*···O4	0.85	1.93	2.760 (3)	167
O3—H3*B*···O39^{vi}	0.85	2.16	2.982 (3)	161
O4—H4*A*···O8	0.85	2.00	2.773 (3)	151
O4—H4*A*···O10	0.85	2.64	3.145 (2)	120
O4—H4*B*···O29^{ix}	0.85	1.80	2.611 (3)	160
O10—H10···O40^{vi}	0.82	1.72	2.5362 (19)	176
O30—H30···O20^{x}	0.82	1.66	2.477 (2)	177

Symmetry codes: (i) −*x*+1, −*y*, −*z*+1; (ii) −*x*+1, −*y*+1, −*z*; (iii) *x*, *y*−1, *z*; (iv) *x*, *y*, *z*−1; (v) *x*−1, *y*, *z*; (vi) −*x*, −*y*+1, −*z*; (vii) −*x*+1, −*y*+1, −*z*+1; (viii) *x*−1, *y*+1, *z*; (ix) *x*, *y*+1, *z*; (x) −*x*+2, −*y*, −*z*+1; (xi) *-x, 2-y, 1-z*; (xii) *x*, *y*, *1+z*.

3.3. The synthesis, molecular and supramolecular structures of $H_2Mf(HpOXA)_2$ anhydrate.

Several techniques such as IR and ^{13}C-CPMAS spectroscopies, X-ray powder diffraction (XRPD), as well as thermal and BET-adsorption analyses were performed in order to elucidate the molecular and supramolecular structure of the microcrystalline anhydrate of formula $H_2Mf(HpOXA)_2$.

The cocrystal $H_2Mf(HpOXA)_2{\cdot}4W$ exhibits a sequence of two weight losses at peak temperatures of 65 °C and 113 °C as endothermic processes, that correspond to the release of one (exp. 2.6%, calcd. 2.7%) and three water molecules (exp. 7.8%, calcd. 8.1%) per formula unit, respectively, Figure 6. The remaining solid is stable between 150 and 200 °C and decomposes at a peak temperature of 212-214 °C, releasing the equivalent to 53% of the initial mass, Figure 5. Thus, a new microcrystalline phase of composition $H_2Mf(HpOXA)_2$ was obtained after air drying at 100 °C, this anhydrate rehydrates into the original tetrahydrate under 100% RH at 40 °C. The XRPD patterns that confirm que crystallinity and change in the solid phases are shown in Figure 7.

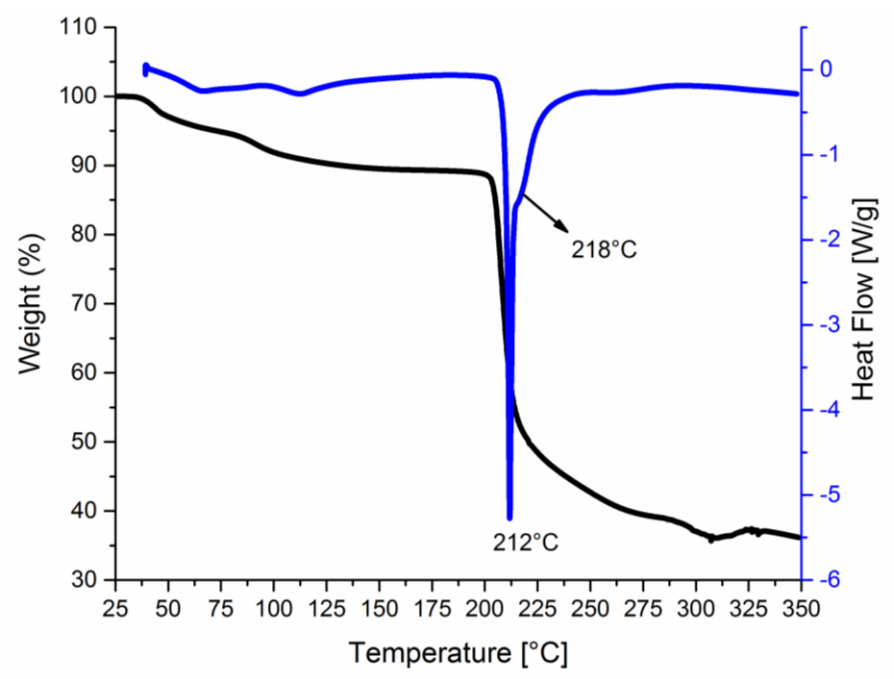

Figure 6. Tg and DSC of $H_2Mf(HpOXA)_2{\cdot}4W$.

Preprints (www.preprints.org) | NOT PEER-REVIEWED | Posted: 27 September 2020 doi:10.20944/preprints202009.0660.v1

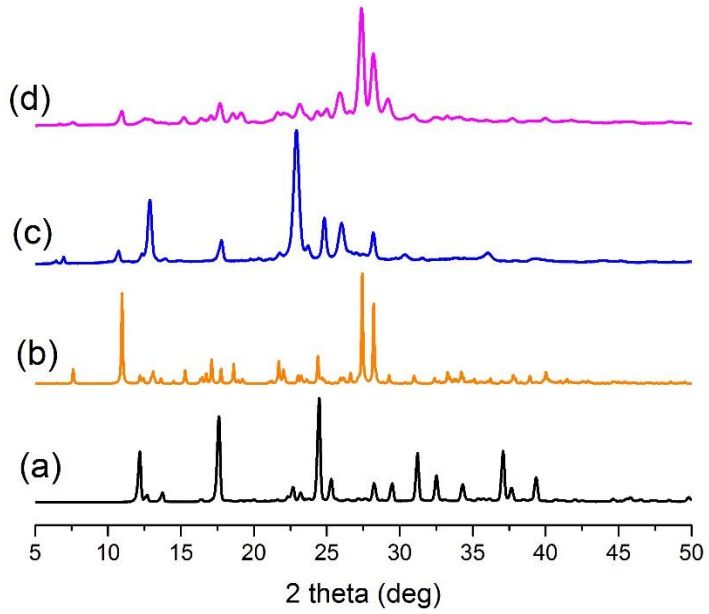

Figure 7. XRPD patterns of: (a) pristine HMfCl, (b) $H_2Mf(HpOXA)_2 \cdot 4W$ cocrystal salt simulated from single crystal X-ray data, (c) $H_2Mf(HpOXA)_2$ microcrystalline powder and (d) after rehydration from $H_2Mf(HpOXA)_2$.

A summary of the IR wavenumbers of $H_2Mf(HpOXA)_2$ tetrahydrate and anhydrate compared to HMfCl are listed in Table 4 and the corresponding IR spectra are shown in Figure 8. The νC=O stretching bands of the carboxylic acid and amide groups as well as the νC=N wavenumbers are red shifted in comparison to the starting $H_2pOXA \cdot 2W$ and HMfCl as a result of hydrogen bonding interactions. As carboxylate group is concerned, it appears at 1524 cm^{-1} in both $H_2Mf(HpOXA)_2$·tetrahydrate and anhydrate, more red shifted than the reported value of 1540 cm^{-1} for the K_2pOXA salt [14] in agreement with highly delocalized structure. It is worth to note that dehydration, considerably clears the spectral window between 3500 to 3000 cm^{-1} allowing the observation of the νN-H bands of the metformin moiety, which are observed in pairs in the IR spectrum of compound $H_2Mf(HpOXA)_2$, but the νN-H bands corresponding to the amide could not be assigned with certainty.

Table 4. Stretching IR absorptions of solid powders of compounds H_2pOXA, HMfCl, $H_2Mf(HpOXA)_2 \cdot 4W$ and $H_2Mf(HpOXA)_2$.

	Bond wavenumber (cm^{-1})			
Comp.	**O—H**	**N—H**	**C=O**	**C=N**
$H_2pOXA \cdot 2W$[a]	3488 (br), 3349 (br)	3335 (m), 3307 (m)	1733 (m), 1714 (m), 1681 (s), 1657 (s)	
HMfCl		3390 (sh), 3379 (m) 3298 (br), 3155 (m) 3095 (sh)		1624 (m), 1584 (sh), 1585 (s), 1550 (s)
$H_2Mf(HpOXA)_2 \cdot 4W$	3442 (br), 3102 (br)	3432 (br), 3358 (br), 3334 (w), 3317 (w)	1686 (vs), 1524 (vs, COO^-)	1672 (sh)
$H_2Mf(HpOXA)_2$	3045 (br, m), 3180 (vw)	3445 (w), 3414 (w) 3372 (w), 3348 (w) 3329 (sh), 3309 (w)	1707 (sh), 1681 (s), 1524 (vs, COO^-)	1650 (sh), 1524 (sh) 1500 (vs)

[a] From reference [14]

Preprints (www.preprints.org) | NOT PEER-REVIEWED | Posted: 27 September 2020 doi:10.20944/preprints202009.0660.v1

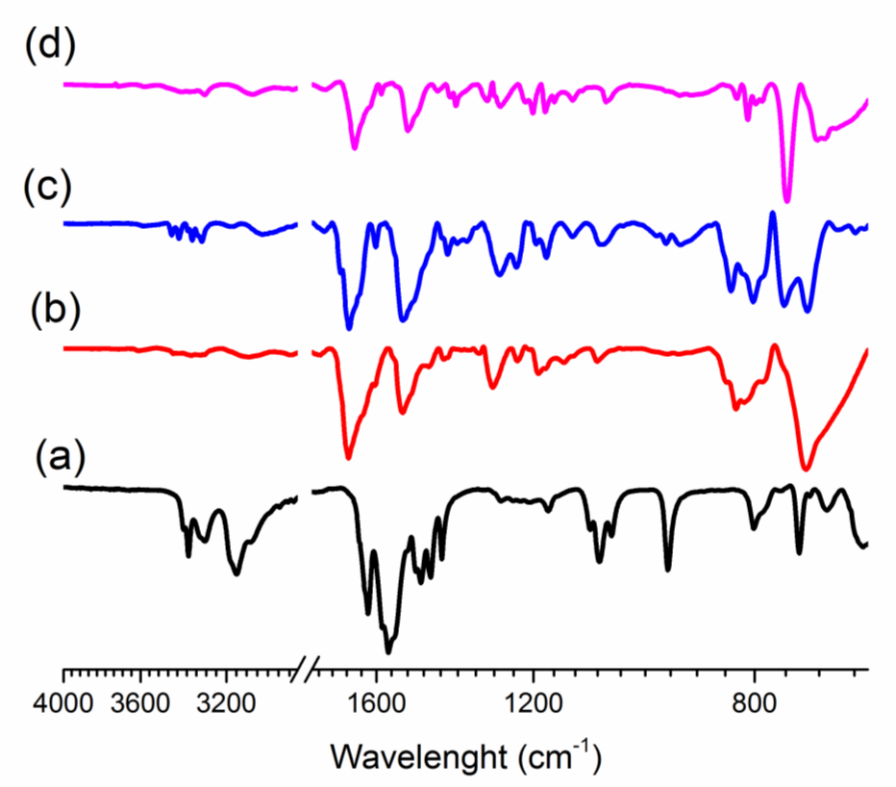

Figure 8. IR spectra of: (a) metformin hydrochloride (HMfCl), (b) $H_2Mf(HpOXA)_2{\cdot}4W$, (c) $H_2Mf(HpOXA)_2$ and (d) $H_2Mf(HpOXA)_2{\cdot}4W$ after rehydration from $H_2Mf(HpOXA)_2$.

On the other hand, the ^{13}C-CPMAS provides useful information regarding the molecular and supramolecular structure. The chemical shift data are listed in Table 5 and spectra are depicted in Figure 9. The chemical shift of the amide carbonyl (C8O) is sensitive to the change in the hydrogen bonding environment, it is spread over 155-159 ppm range, in response to the hydrogen bonding scheme in the crystal lattice of $H_2Mf(HpOXA)_2{\cdot}4W$ cocrystal. Whereas both COOH and COO^- groups appear as one signal slightly shifted by ~ 2 ppm to high frequencies compared to the starting $H_2pOXA{\cdot}2W$. This result is similar to that found in other carbonyls because of hydrogen bonding [31]. The *sp-sp* disposition between both oxalyl groups, in relation to the phenyl plane, and the presence of two independent molecules of $HpOXA^-$ in the asymmetric unit, as well as hydrogen bonding, have the effect to spread the CH signals of the benzene ring in the 121-118 ppm range. The loss of water molecules opens the spectral window from 123 to 117 ppm and shifts the amide carbonyl to low frequencies by ~ 2 ppm. The chemical shifts of the dicationic metformin moieties, in both tetrahydrate and anhydrate cocrystals of $(H_2Mf)(HpOXA)_2$, are the same as those observed in the monocationic HMfCl, except that the value of the carbon atom in the $C(NH_2)NMe_2$ fragment is shifted by ~ 2 ppm to high frequencies, in agreement with increased delocalization and positive charge (vide supra). The analysis of the vibrational spectra and ^{13}C-CPMAS NMR data of $H_2Mf(HpOXA)_2{\cdot}4W$ and its anhydrate suggests that their structures, conformation and hydrogen bonding schemes of both cocrystals are very similar between them, with the exception of those regions formerly occupied by water molecules. Rehydration experiments performed on the $H_2Mf(HpOXA)_2$ anhydrate, which reversibly rehydrates to the tetrahydrate, support these findings.

Preprints (www.preprints.org) | NOT PEER-REVIEWED | Posted: 27 September 2020 doi:10.20944/preprints202009.0660.v1

Table 5. CPMAS and isotropic ^{13}C chemical shifts of H_2pOXA, HMfCl, H_2Mf(HpOXA)$_2$·4W and H_2Mf(HpOXA)$_2$.

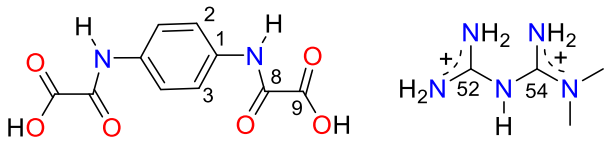

Comp	C1	C2	C3	C8O	C9O	C52	C54	CH$_3$
H_2pOXA[a]	134.6	121.0	121.0	157.1	162.6			
HMfCl[a]						158.9	159.6	37.9
HMfCl crystals						159	162	42, 40
(H_2Mf)(HpOXA)$_2$·4W	136[b]	120	121[b]	159[b]	164[d]	159	160	42, 40
	134, 132	118[c]	120[c]	155[b]				
(H_2Mf)(HpOXA)$_2$	136	119, 118[b]	123	157	164	159	160	42, 41
	134[c]	117	120[c]	154	163			

[a] in DMSO-d6 solution; [b] 2C; [c] 3C; [d] 4C

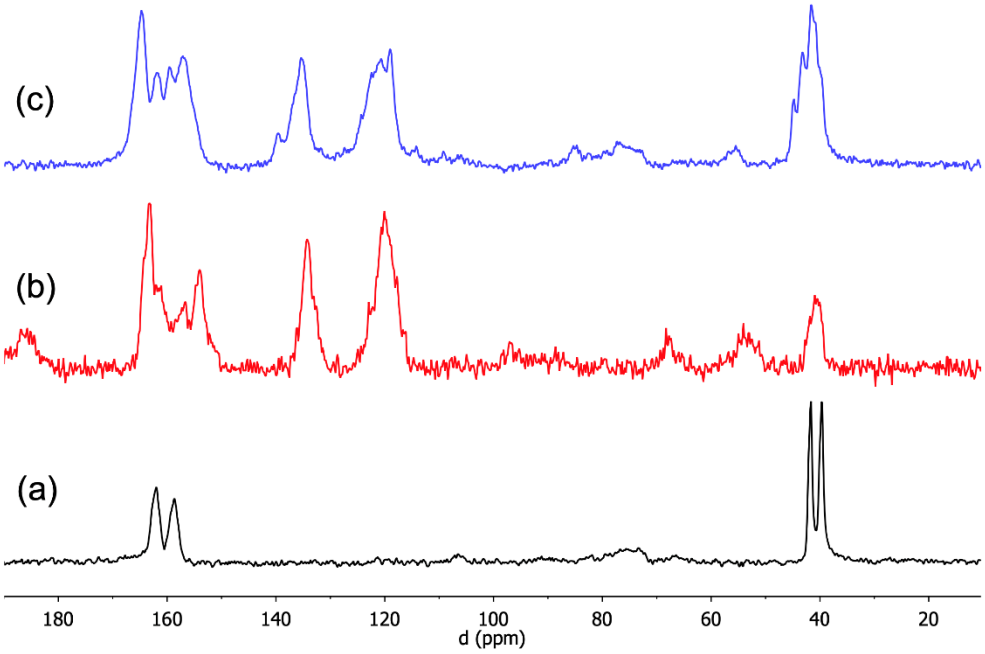

Figure 9. ^{13}C-CPMAS (a) pristine HMfCl, (b) H_2Mf(HpOXA)$_2$·4W cocrystal salt and (c) H_2Mf(HpOXA)$_2$ microcrystalline powder.

Rehydration experiments performed on the H_2Mf(HpOXA)$_2$·anhydrate, which reversibly rehydrates to the tetrahydrate H_2Mf(HpOXA)$_2$·4W, support the above findings. Furthermore, dehydration of H_2Mf(HpOXA)$_2$·4W can be associated with the role of water molecules in its crystal structure. As mentioned before, it occurred in two steps: one water molecule is lost at 65 °C followed by three more at 113 °C before decomposition. Judging by the number of hydrogen bonds and their strength, the water molecule labelled as W2 can be assigned to the first loss; it is forming strong hydrogen bonds with amide and metformin NH in the crystal as well as acting as a bridge between two $HpOXA^-$ moieties of parallel chains, see Figure 5. Whereas, the water molecules labelled as W1, W3 and W4 form similar hydrogen bonds in number and nature as W2, but they are clustered together (*vide supra*) and therefore leaving the crystal lattice at higher temperature. The removal of all water molecules from the isolated pockets of H_2Mf(HpOXA)$_2$·4W, results in a stable framework given by the ionic interactions of the H_2Mf^{2+} dication and two units of the $HpOXA^-$ monoanion. This framework is stable and capable to rearrange in the presence of moisture, restoring the

Preprints (www.preprints.org) | NOT PEER-REVIEWED | Posted: 27 September 2020 doi:10.20944/preprints202009.0660.v1

microcrystalline lattice of the original tetrahydrate. A similar behavior has been observed in sitafloxacin hydrate [32]. The formation of microporous channels in the structure of $H_2Mf(HpOXA)_2$ was disregarded with a BET adsorption experiment, Figure 10(a), which resulted in type III isotherm, characteristic of mesoporous solids, with pore size of ~ 16 nm and surface area of 7.7 $m^2\ g^{-1}$. The formation of large pores is in agreement with the ordered water detach from the crystal structure, making available space along which water can diffuse in during rehydration. Thus, the main role of the water in the crystal lattice of $H_2Mf(HpOXA)_2{\cdot}4W$ is proposed not only to compensate the excess of donors given by the metformin moiety, but also to provide the hydrogen bonding interactions to build the third dimension in the crystal lattice. The examination of the $H_2Mf(HpOXA)_2{\cdot}4W$ crystal lattice allows us to propose that most of the original hydrogen bonding interactions as well as n→π* charge-assisted interactions in the (0 1 1) plane are preserved after dehydration. Whereas the (1 1 -1) plane is weakened after water loss, to form the $H_2Mf(HpOXA)_2$ mesoporous solid phase, Figure 10(b).

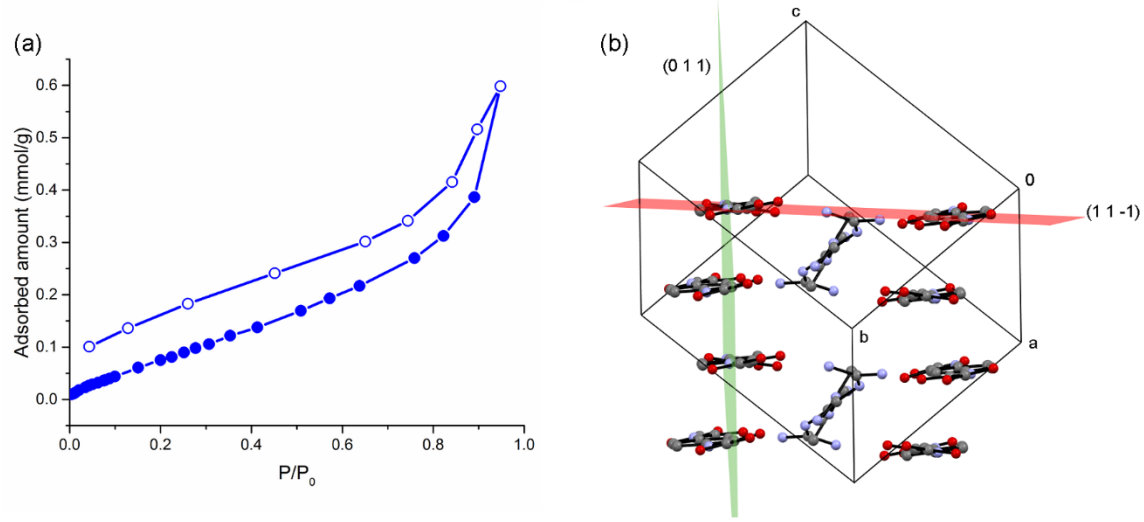

Figure 10. (a) BET isotherm of $H_2Mf(HpOXA)_2$, hollow squares for adsorption and solid circles for desorption. (b) View of the $H_2Mf(HpOXA)_2{\cdot}4W$ planes, water molecules are omitted. The hydrogen bonding network is weakened in the (1 1 -1) plane, but hydrogen bonding and n→π* charge-assisted interactions prevail in the (0 1 1) plane.

3.4. The nature and structure of dicationic metfomin in $H_2Mf(HpOXA)_2{\cdot}4W$ and $H_2Mf(HpOXA)_2$ cocrystal salts.

Metformin behaves as diprotic acid whose pKa values are referred here as pK_{a1} and pK_{a2}, corresponding to H_2Mf^{2+}/HMf^{+} and HMf^{+}/Mf acid-base conversions, respectively. The reported pK_a values are spread over a wide range depending upon the experimental method of measurement [33]. The pK_{a1} and pK_{a2} values are reported in between 0.7-3.1 and 11.5-15.3 intervals, respectively. The formation of the salt cocrystal $H_2Mf(HpOXA)_2{\cdot}4W$, *vide supra*, is explained by the proton transfer from H_2pOXA, as the acid, to HMf^{+}, as the base. The ΔpKa rule stablishes that ionized acid-base molecular complexes, in the solid phase, are observed exclusively for ΔpKa > 4 [34]. The ΔpKa is the difference between the pKa of the base and the pKa of the acid. Therefore, the ΔpKa rule lead us to estimate the pK_{a1} value for the first deprotonation event of H_2pOXA in the -3.3 to -0.9 range, corresponding to a strong acid.

Furthermore, the protonation of the nitrogen bridge, in dicationic metformin, avoids the formation of the homodimer $R^2_2(8)$, raised by N—H···N interactions. This motif is frequently observed in the crystal structures of the monocationic metformin salts but absent in all dicationic known salts of metformin [6] including the tetrachlorocuprate [35]. Instead, a hydrogen bonding heterodimer $R^a_d(n)$ is formed in dicationic salts, with the participation of the anion group: $R^2_2(8)$ in the oxalic acid [29] and nitrate [36], $R^2_2(9)$ in squarate [37] and oxalamate monoacid (this work),

Preprints (www.preprints.org) | NOT PEER-REVIEWED | Posted: 27 September 2020 doi:10.20944/preprints202009.0660.v1

$R^3_3(12)$ motif in sulfate [29] and $R^2_2(16)$ in sulfonatocalix[4,5]arenes [38]. The conformation in the form of an S backbone and the strongest acid on the nitrogen bridge seems to favor the hetero- over the homo-association. At this point, it is worth to highlight the differences between metformin-carboxylate and metformin-oxalamate salts. The first forms the hydrogen bonding hetero-dimeric $R^2_2(8)$ motif, which has been found, in the crystal network of guanidinium–carboxylate synthons [9]. This dominant motif is absent in the oxalamate salt $H_2Mf(HpOXA)_2{\cdot}4W$. Instead, the amide carbonyl of the $HpOXA^-$ moiety participates in the formation of the observed $R^2_2(9)$ motif and in the n→ π* charge-assisted interactions of mono-and bifacial type, herein described (see Table 2). Even weak in strength, the n→ π* interaction, also named as π-hole, has been found important for the stability of biomolecules and materials [39]. Because of the nature and bonding of the atoms involved, the carbonyl-guanidinium synthon CO···CN^+, is similar to CO···CO interactions [30], but charge assisted. This synthon as well as H_2O···CN^+ synthon are present, even when not described in the original sources, in the crystal network of metformin dicationic salts of squarate and oxalate. The analogous synthon SO···CN was identified in the crystal network of the acesulfame [40] and also in sulfonatocalix[4,5]arene metformin dicationic salts, in this last in the bifacial fashion SO···CN^+···OS. Selected geometric parameters are listed in Table 6, to support the above discussion.

Table 6. Geometric parameters of regular O(δ-)···C(δ+) and bifacial O(δ-)···C(δ+)···O(δ-) n→ π* interactions reported in H_2MfA cocrystal salts (A = anion).

Cocrystal	X—O···C	XO···C/Å	X—O···C/°	O···C···O /°	Me_2NCNC/°
$H_2Mf(HpOXA)_2$ (this work)	CO···C54	3.142(3)	133.4(2)		148.8(2)
	CO···C54	3.109(3)	131.8(2)	163.6(3)	
H_2Mf-squarate (1)[a]	CO···C	3.212	148.0		-144.9
	H_2O···C	3.156	167.5	136.3	
H_2Mf-squarate (2)[a]	CO···C	2.988	87.9		143.3
	CO···C	3.023	87.7		
H_2Mf-oxalate[b]	CO···C	3.108	88.9		143.2
	H_2O···C	3.152	158.3		
H_2Mf-sulfonatocalix[4,5]arenes[c]	SO···C	2.938	132.2		41.4
	SO···C	3.187	148.0	163.0	
H_2Mf-acesulfame[d]	SO···C	3.130	128.1		141.6

[a][37], [b][29] [c][38], [d][40]

It has been revealed that the n→π* interaction can modulate the overall structural motifs even in the presence of strong hydrogen bonding interactions [41]. The results herein described for recurrent n→π* charge-assisted interactions of mono-and bifacial type, in dicationic metformin salts, support the existence of these interactions independently, and not just as a short contact imposed by the geometric constraint due to the hydrogen bonding patterns. This O(δ-)···C(δ+) and O(δ-)···N^+ could be responsible of the interactions of metformin in biologic systems.

4. Conclusions

The $H_2Mf(HpOXA)_2{\cdot}4W$ framework is given by ionic interactions of the H_2Mf^{2+} dication and two units of the $HpOXA^-$ monoanion. The inherent flexibility of both components is lost by the strong hydrogen bonding and n→π* charge-assisted interactions between both moieties whereas the main role of the water molecules is to equilibrate the number of hydrogen acceptors in the crystal network. The vacant pockets left behind after water removal are preserved in the $H_2Mf(HpOXA)_2$ anhydrate, whose crystal network is stable and capable to rearrange in the presence of moisture to restore the microcrystalline lattice of the original tetrahydrate under proper conditions.

The formation of the salt cocrystal $H_2Mf(HpOXA)_2{\cdot}4W$ implies the proton transfer from H_2pOXA, as the acid, to HMf^+, as the base. The first deprotonation event of H_2pOXA was estimated

in the -3.3 to -0.9 range, corresponding to a medium strength acid. The structure of metformin in the 1:2 cocrystal salt $H_2Mf(HpOXA)_2{\cdot}4W$ is very similar to that observed in the monohydrates of the two other known dicationic 1:1 salts of formula $(H_2Mf)A{\cdot}H_2O$ (A = oxalate, sulfate). The conformation in the form of an S backbone and the strongest acid on the nitrogen bridge seems to favor the hetero- over the homo-association, therefore dicationic metformin is prone to hydrogen bonding with anions to form hetero $R^a_d(n)$ motifs. The *syn* conformation adopted by the *N*,*N*′-(1,4-phenylene)dioxalamic acid is uncommon among organic cocrystals but only attained by coordination to metals. The amide carbonyl of the $HpOXA^-$ moiety participates in the formation of the observed $R^2_2(9)$ motif and in the n→π* charge-assisted interactions of mono-and bifacial type.

Author Contributions: Conceptualization, I.I.P.-M. and F.J.M.-M.; methodology, S.C.-C., A.A.R.-O.; formal analysis, S.C.-C. and E.V.G.-B.; writing—original draft preparation, S.C.-C., F.J.M.-M. and I.I.P.-M.; writing—review and editing and funding acquisition, I.I.P.-M. All authors have read and agreed to the published version of the manuscript.

Funding: This research was funded by CONACYT, grant number 255354 and Secretaría de Investigación Posgrado del Instituto Politécnico Nacional, grant number 20170504.

Acknowledgments: This work was supported by CONACYT Grant 255354, SIP-IPN Grant 20170504 (Secretaria de Investigación y Posgrado del Instituto Politécnico Nacional), CONACYT´ "Red Tematica de Química Supramolecular" Grant 271884. CGIC-UC (Coordinación General de Investigación Científica de la Universidad de Colima) and PROMEP-SEP. S.C.-C. thanks CONACYT for fellowship and I.I.P.-M. thanks Dr. Susana Rojas-Lima of UAEH for the access to the X-ray diffractometer.

Conflicts of Interest: The authors declare no competing financial interest.

Orcid:

Itzia I. Padilla-Martínez: 0000-0002-9645-2049

Efrén V. García-Báez: 0000-0003-0920-7385

Francisco J. Martínez-Martínez: 0000-0001-6951-9837

Sayuri Chong Canto: 0000-0001-5411-0748

Angel Ramos Organillo: 0000-0002-9690-608X

References

1. Shan, N.; Zaworotko, M.J. The role of cocrystals in pharmaceutical science. *Drug Discovery Today* **2008**, *13*, 441-446.
2. Das, P.; Delost, M.D.; Qureshi, M.H.; Smith, D.T.; Njardarson, J.T. A Survey of the Structures of US FDA Approved Combination Drugs. *J. Med. Chem.* **2019**, *62*, 4265−4311.
3. Bian, X.; Jiang, L.; Gan, Z.; Zhang, L., Cai, L.; Hu, X. A Glimepiride-Metformin Multidrug Crystal: Synthesis, Crystal Structure Analysis, and Physicochemical Properties. *Molecules* **2019**, *24* 3786.
4. Bhatt, J.A.; Bahl, D.; Morris, K.; Stevens, L.L.; Haware, R.V. Structure-mechanics and improved tabling performance of the drug-drug cocrystal metformin-salicylic acid. *Eur J Pharm Biopharm* **2020**, *153*, 23-35.
5. Plata-Vargas, E.; de la Cruz-Hernández, C.; Dorazco-González, A.; Fuentes-Noriega, I.; Morales-Morales, D.; Germán-Acacio, J.M. Synthesis of Metforminium Succinate by Melting. Crystal Structure, Thermal, Spectroscopic and Dissolution Properties. *J. Mex. Chem. Soc.* **2017**, *61*, 197-204.
6. Kathuria, D.; Bankar, A.A.; Bharatam, P.V. What's in a structure? The story of biguanides. *Molecular Structure* **2018**, *1152*, 61-78.
7. Hariharan, M.; Rajan, S.S.; Srinivasan, R. Structure if metformin hydrochloride. *Acta Cryst.* **1989**, *C45*, 911-913.
8. Childs, S.L.; Chyall, L.J.; Dunlap, J.T.; Coates, D.A.; Stahly, B.C.; Stahly, G.P. A Metastable Polymorph of Metformin Hydrochloride: Isolation and Characterization Using Capillary Crystallization and Thermal Microscopy Techniques. *Cryst. Growth Des.* **2004**, *4*, 441-449.
9. Nanubolu, J.B.; Sridhar, B.; Ravikumar, K.; Sawant, K.D.; Naik, T.A.; Patkar, L.N.; Cherukuvada, S.; Sreedhar, B. Polymorphism in metformin embonate salt - recurrence of dimeric and tetrameric guanidinium-carboxylate synthons. *CrystEngComm* **2013**, *15*, 4448-4464.

10. González-González, J.S.; Martínez-Martínez, F.J.; García-Báez E.V.; Cruz, A.; Morín-Sánchez, L.M.; Rojas-Lima, S.; Padilla-Martínez, I.I. Molecular Complexes of Diethyl N,N′-1,3-Phenyldioxalamate and Resorcinols: Conformational Switching through Intramolecular Three-Centered Hydrogen-Bonding. *Cryst. Growth Des.* **2014**, *14*, 628-642.
11. Hall, C.M.; Wright, J.B. Antiallergic phenylenedioxamic acids. *Ger. Offen.* **1974**, DE 2362409 A1 19740627.
12. Wright, J.B.; Hall, C.M.; Johnson, H.G.J. N,N'-(phenylene)dioxamic acids and their esters as antiallergy agents. *Med. Chem.* **1978**, *21*, 930-935.
13. Petyunin, G.P. Synthesis and pharmacological activity of phenylenedioxamic acids. *Khimiko-Farmatsevticheskii Zhurnal* **1986**, *20*, 827-830.
14. Oliveira, W.X.C.; Pinheiro, C.B.; da Costa, M.M.; Fontes, A.P.S.; Nunes, W.C.; Lloret, F.; Julve, M.; Pereira, C.L.M. Crystal Engineering Applied to Modulate the Structure and Magnetic Properties of Oxamate Complexes Containing the [Cu(bpca)]+ Cation. *Cryst. Growth Des.* **2016**, *16*, 4094−4107.
15. Lisnard, L.; Chamoreau, L.-M.; Li, Y.; Journaux, Y. Solvothermal Synthesis of Oxamate-Based Helicate: Temperature Dependence of the Hydrogen Bond Structuring in the Solid. *Cryst. Growth Des.* **2012**, *12*, 4955−4962.
16. Ramírez-Milanés, E.G.; Martínez-Martínez, F.J.; Magaña-Vergara, N.E.; Rojas Lima, S.; Avendaño-Jiménez, Y.A.; García-Báez, E.V.; Morín-Sánchez, L.M.; Padilla-Martínez, I.I. Positional isomerism and steric effects in the self-assemblies of phenylene bis-monothiooxalamides. *Cryst. Growth Des.* **2017**, *17*, 2513-2528.
17. Gómez-Castro, C.Z.; Padilla-Martínez, I.I.; García-Báez, E.V.; Castrejón-Flores, J.L.; Peraza-Campos, A.L.; Martínez-Martínez, F.J. Solid state structure and solution thermodynamics of the three-centered hydrogen bond (O···H···O) using N-(2-benzoylphenyl) oxalyl derivatives as model compounds. *Molecules* **2014**, 19, 14446-14460.
18. Cabrera-Pérez, L.C.; García-Báez, E.V.; Franco-Hernández, M.O.; Martínez-Martínez, F.J.; Padilla-Martínez, I.I. Carbonyl–carbonyl interactions and amide π-stacking as the directing motifs of the supramolecular assembly of ethyl N-(2-acetylphenyl)-oxalamate in a synperiplanar conformation. *Acta Cryst.* **2015**, *C71*, 381-385.
19. Martin, S.; Beitia, J.I.; Ugalde, M.; Vitoria, P.; Cortes, R. Diethyl N,N'-o-phenylenedioxamate. *Acta Crystallographica, E: Structure Reports Online* **2002**, *58*, o913-o915.
20. James, S. L.; Adams, C. J.; Bolm, C.; Braga, D.; Collier, P.; Friščić, T.; Grepioni, F.; Harris, K. D. M.; Hyett, G.; Jones, W.; Krebs, A.; Mack, J.; Maini, L.; Orpen, A. G.; Parkin, I. P.; Shearouse, W. C.; Steedk, J. W.; Waddelli, D. C. Mechanochemistry: opportunities for new and cleaner synthesis. *Chem. Soc. Rev.* **2012**, *41*, 413–447.
21. CrysAlis PRO, Agilent Technologies: Yarnton, UK, **2012**.
22. Sheldrick, G.M. A short History of SHELX. *Acta Cryst.* **2007**, *A64*, 112–122.
23. Farrugia, L.J., WinGX and ORTEP for windows: An update. *J. Appl. Cryst.* **2012**, *45*, 849-854.
24. Spek, A.L., Structure validation in chemical crystallography. *Acta Cryst.* **2009**, *D65*, 148-155.
25. Macrae, C.F.; Bruno, I.J.; Chisholm, J.A.; Edgington, P.R.; McCabe, P.; Pidcock, E.; Rodriguez-Monge, V.; Taylor, R.; van de Streek, J.; Wood, P.A., Mercury CSD 2.0 - New Features for the Visualization and Investigation of Crystal Structures. *J. Appl. Cryst.* **2008**, *41*, 466-470.
26. Pardo, E.; Cangussu, D.; Lescouezec, R.; Journaux, Y.; Pasan, J.; Delgado, F.S.; Ruiz-Pérez, C.; Ruiz-García, R.; Cano, J.; Julve, M.; Lloret, F., Molecular-Programmed Self-Assembly of Homo- and Heterometallic Tetranuclear Coordination Compounds: Synthesis, Crystal Structures, and Magnetic Properties of Rack-Type CuII2MII2 Complexes (M = Cu and Ni) with Tetranucleating Phenylenedioxamato Bridging Ligands. *Inorganic Chemistry* **2009**, *48*, 4661-4673.
27. Devi, R.N.; Jelsch, C.; Israel, S.; Aubert, E.; Anzline, C.; Hosamani, A.A., Charge density analysis of metformin chloride, a biguanide anti-hyperglycemic agent. *Acta Cryst.* **2017**, *B73*, 10–22.
28. Allen, F.H.; Kennard, O; Watson, D.G.; Brammer, L.; Orpen, A.G.; Taylor, R., Tables of bond lengths determined by x-ray and neutron diffraction. Part 1. Bond lengths in organic compounds. *J. Chem. Soc., Perkin Trans. 2* **1987**, *12*, S1-S19.
29. Lu, L.P.; Zhang, H.M.; Feng, S.S.; Zhu, M.L. Two N,N-dimethylbiguanidium salts displaying double hydrogen bonds to the counter-ions. *Acta Cryst.* **2004**, *C60*, o740-o743.
30. Allen, F. H.; Baalham, C. A.; Lommerse, J. P. M.; Raithby, P. R. Carbonyl-Carbonyl Interactions can be Competitive with Hydrogen Bonds. *Acta Cryst.* **1998**, *B54*, 320-329.

31. Kashid, S.M.; Sayan, B. Experimental Determination of the Electrostatic Nature of Carbonyl Hydrogen-Bonding Interactions Using IR-NMR Correlations. *J. Phys. Chem. Lett.* **2014**, *5*, 3211−3215.
32. Suzuki, T.; Araki, T.; Kitaoka, H.; Terada, K. Characterization of Non-stoichiometric Hydration and the Dehydration Behavior of Sitafloxacin Hydrate. *Chem. Pharm. Bull.* **2012**, *60*, 45—55.
33. Langmaier, J.; Pižl, M.; Samec, Z.; Záliž, S. Extreme Basicity of Biguanide Drugs in Aqueous Solutions: Ion Transfer Voltammetry and DFT Calculations. *Journal of Physical Chemistry A* **2016**, *120*, 7344-7350.
34. Cruz-Cabeza, A.J. Acid–base crystalline complexes and the pKa rule. *CrystEngComm* **2012**, *14*, 6362–6365.
35. Lemoine, P.; Tomas, A. Tétrachlorocuprate(II) de metformine. *Acta Cryst.* **1994**, *C50*, 1437-1439.
36. Fridrichová, M.; Císařová, I.; Němec, I. 1,1-Dimethylbiguanidium(2+) dinitrate. *Acta Cryst.* **2012**, *E68*, o18–o19.
37. Şerb, M.D.; Kalf, I.; Englert, U. Biguanide and squaric acid as pH-dependent building blocks in crystal engineering. *CrystEngComm* **2014**, *16*, 10631-10639.
38. Guo, D.S.; Zhang, H.Q.; Ding, F.; Liu, Y. Thermodynamic origins of selective binding affinity between *p*-sulfonatocalix[4,5]arenes with biguanidiniums. *Org. Biomol. Chem.* **2012**, *10*, 1527–1536.
39. Bauzá, A.; Mooibroek, T.J.; Frontera, A. The Bright Future of Unconventional s/p-Hole Interactions. *ChemPhysChem* **2015**, *16*, 2496–2517.
40. Wang, C.; Hu, S.; Sun, C.C. Expedited development of a high dose orally disintegrating metformin tablet enabled by sweet salt formation with acesulfame. *Int. J. Pharmaceutics* **2017**, *532*, 435–443.
41. Singh, S, K.; Das, A., The n-π* interaction: a rapidly emerging non-covalent interaction. *Phys. Chem. Chem. Phys.* **2015**, 17, 9596—9612.